Dominant Mobility Modulation by the Electric Field Effect at the $LaAlO_3/SrTiO_3$ Interface

C. Bell,[1,2] S. Harashima,[1] Y. Kozuka,[1] M. Kim,[1] B. G. Kim,[1,3] Y. Hikita,[1] and H. Y. Hwang[1,2]

[1]*Department of Advanced Materials Science, University of Tokyo, Kashiwa, Chiba 277-8651, Japan*
[2]*Japan Science and Technology Agency, Kawaguchi, 332-0012, Japan*
[3]*Department of Physics, Pusan National University, Busan 609-735, Korea*
(Received 15 March 2009; published 24 November 2009)

Caviglia *et al.* [Nature (London) **456**, 624 (2008)] have found that the superconducting $LaAlO_3/SrTiO_3$ interface can be gate modulated. A central issue is to determine the principal effect of the applied electric field. Using magnetotransport studies of a gated structure, we find that the mobility variation is almost 5 times that of the sheet carrier density. Furthermore, superconductivity can be suppressed at both positive and negative gate bias. These results indicate that the relative disorder strength strongly increases across the superconductor-insulator transition.

DOI: 10.1103/PhysRevLett.103.226802 PACS numbers: 73.20.−r, 85.30.Tv

The strength of the electric field effect (EFE) in accumulating or depleting carriers in a conducting channel is central not only to many semiconductor devices found ubiquitously in modern electronics, but also in current research into achieving novel physics using tunable materials. Complex oxides are one case where the electronic ground state of the system is highly sensitive to the carrier density [1,2]. Among the commonly studied oxide materials, $SrTiO_3$ has attracted much attention due to its high electron mobility and electric permittivity at low temperatures, which facilitates large electric field effects [3]. Many recent oxide EFE devices have utilized $SrTiO_3$ substrates as a crucial component of the experiment: both the metallicity and superconductivity of $SrTiO_3$ have been modulated [2,4–6].

Recently, Caviglia *et al.* [2] strikingly demonstrated that the EFE could be used to modulate the superconductivity which appears [7] in the metallic gas formed between the two insulators $LaAlO_3$ and $SrTiO_3$. Since its first discovery [8], the origin and physics of this metallic layer has been intensively investigated. Room temperature scanning electron energy-loss spectroscopy and conducting scanning probe measurements have set an upper limit of $\sim$7 nm for the gas thickness in annealed or high pressure grown samples [9,10]. However, it is still unclear how the gas thickness is correlated to the sheet resistance at low temperatures, which itself can be changed by several orders of magnitude with oxygen pressure during $LaAlO_3$ growth [8,11], or the EFE [2,5].

In this context, Caviglia *et al.* assumed that the superconductivity suppression by the EFE is due to the reduction of the carrier density of the electron gas. However, it was unclear how the mobility of the electron gas changed in these initial EFE experiments, since it was not probed. A direct measurement of the mobility is vital in order to experimentally determine what is the effective tuning parameter of the superconductor-insulator transition. In this Letter, we describe a detailed study of the magnetotransport properties of a $LaAlO_3/SrTiO_3$ interface, for which superconductivity can be fully suppressed by both positive and negative gate bias. Normal-state magnetotransport measurements were also made above the upper critical field at which superconductivity is destroyed. From these data, we find that not only does the carrier density vary with applied gate voltage, but a significant change of the electron mobility also occurs, with the latter dominating the change in the normal-state conductivity. These results are crucial for a full understanding of the nature of the transition from the superconducting to insulating state in this system, and others like it which utilize $SrTiO_3$ as an active element [3–6,12–14].

Our sample was grown by pulsed laser deposition as described elsewhere [15] using an oxygen pressure of 1.33×10^{-3} Pa. The $LaAlO_3$ thickness was 10 unit cells, as monitored using *in situ* reflection high-energy electron diffraction. The substrate was 5 mm $\times$ 5 mm $\times$ 0.5 mm $SrTiO_3$ (100) with a TiO_2 terminated surface. Using optical lithography, a six contact Hall bar (central bar length 500 μm, width 100 μm) was patterned onto the $SrTiO_3$ utilizing amorphous AlO_x as a hard mask, which was lift-off patterned at room temperature prior to the $LaAlO_3$ growth.

The Hall bar was ultrasonically wirebonded with Al wire to form Ohmic contacts, and the gate contact was made on the back of the $SrTiO_3$ substrate via conducting silver epoxy. A quasi dc bias current sweep between 1–100 nA was used for all transport measurements. The back gate leakage current was <0.1 nA for all temperatures and voltages. Sheet resistance versus temperature, $R(T)$, was measured in the temperature range 0.05 K $\leq T \leq$ 0.5 K in a dilution refrigerator with a base temperature of 10 mK. The gate voltage V_g was first swept between the maximum and minimum values of ± 100 V to remove history effects [2], before measurements were made at 25 V intervals. Similar measurements were also performed in a helium-4 cryostat for 2 K $\leq T \leq$ 300 K, which was more conve-

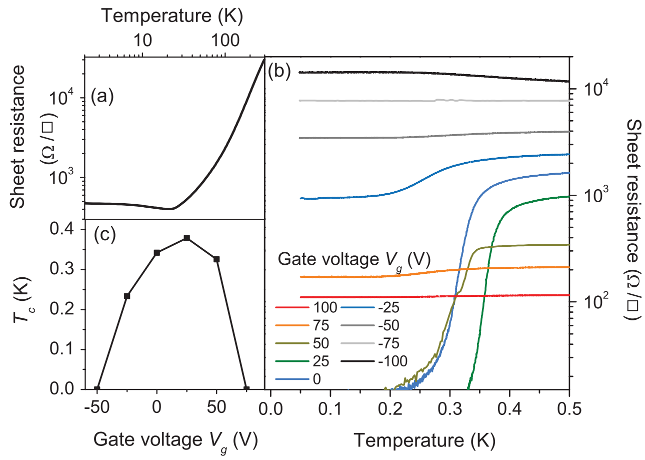

FIG. 1 (color). (a) $R(T)$ from $T = 300$ K before biasing. (b) Low temperature $R(T)$ for various gate voltages. (c) Superconducting critical temperature T_c versus gate voltage.

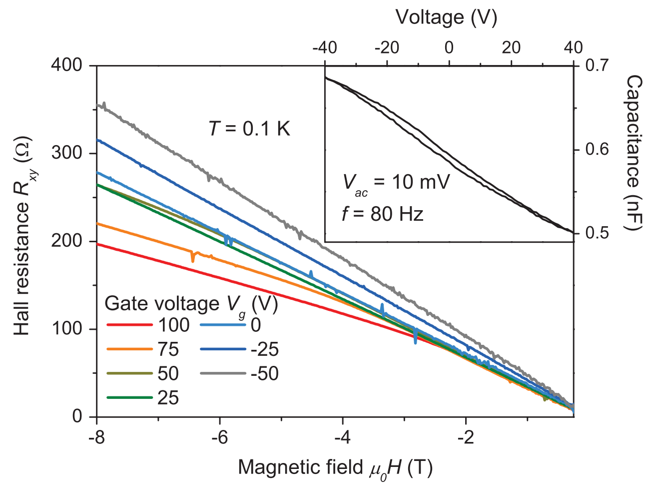

FIG. 2 (color). Antisymmetrized Hall resistance versus magnetic field, $R_{xy}(H)$ for various V_g at $T = 0.1$ K. Lines are guides to the eye. Inset: Capacitance versus voltage at $T = 0.1$ K.

nient to investigate thermal history effects associated with changes in V_g.

Figure 1(a) shows $R(T)$ in the high temperature regime before applying a gate voltage, showing a slight upturn around $T = 20$ K, similar to that observed elsewhere [7,8,11]. Figure 1(b) shows the low temperature $R(T)$ for various V_g applied. A clear systematic increase of the resistance is observed for $V_g < 0$ and decrease for $V_g > 0$. Superconductivity is found for the range $-50\ \text{V} < V_g < 75$ V, with $T_c = 378$ mK at $V_g = +25$ V, as shown in the phase diagram of Fig. 1(c). Here, for simplicity, we have defined T_c as the temperature at which the sheet resistance falls below 50% of the value at $T = 0.5$ K. Similar to Ref. [2], we can completely suppress T_c by applying a negative gate voltage (removing electrons), but in this sample, we can also add electrons (positive V_g) and reduce T_c to zero.

The normal-state magnetotransport properties were measured above the superconducting upper critical field, H_{c2}, using a magnetic field $\mu_0 H \gg 150\ \text{mT} > \mu_0 H_{c2}$. The Hall resistance data at $T = 0.1$ K are shown in Fig. 2. The extracted sheet carrier density, $n_{2d} \sim 1.8 \times 10^{13}\ \text{cm}^{-2}$ for $V_g = 0$ V at $\mu_0 H = 2$ T is comparable to other studies. Applying positive V_g, $R_{xy}(H)$ develops a nonlinearity; hence, we extract the sheet carrier density from the Hall coefficient at both 8 and 2 T. At $V_g = -75$ and -100 V, $R_{xy}(H)$ could not be measured reliably, suggesting that inhomogeneities develop in the wire at higher sheet resistances. The carrier density modulation for both high (8 T) and low (2 T) field fits show the same trend with V_g: a reduction of ~45% between $V_g = +100$ and -50 V (Fig. 3). The modulation of the sheet carrier density in this voltage range is linear, meaning that the device is operating as a conventional metal oxide field effect transistor. Measurements at $T = 2$ K show a similar trend, with only a slight difference in the value of n_{2d}.

The relative change in charge with V_g can also be estimated using the integrated capacitance versus voltage ($C(V_g)$, inset Fig. 2). However, we found that the charge variation, as scaled by the area of the Hall bar, was significantly larger than that measured by the Hall effect (n_{c1} data in Fig. 3). We find better agreement with the Hall effect by scaling with the bottom gate area (n_{c2}, Fig. 3); however, this would imply some conduction beneath the AlO_x hard mask, despite the large measured resistance $>100\ \text{G}\Omega/\square$. The clear hysteresis observed in the $C(V_g)$ data (inset Fig. 2), which was insensitive to frequency in the range of 40–640 Hz with different voltage sweep rates, suggests the presence of weak induced interfacial ferroelectricity due to the presence of a large electric field

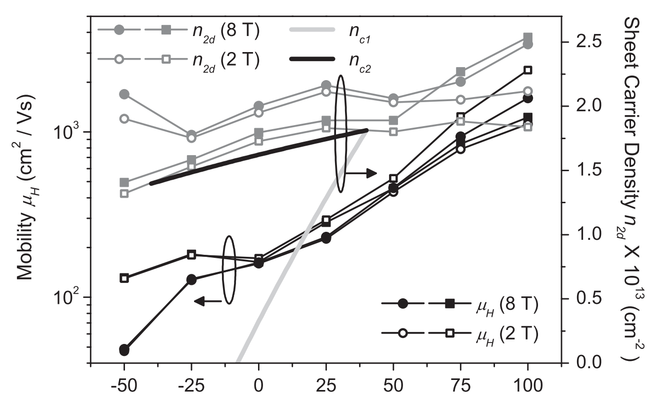

FIG. 3. Sheet carrier density n_{2d} and electron mobility μ_H versus V_g, at $T = 0.1$ K (squares) and $T = 2$ K (circles). Closed and open symbols refer to high field (8 T) and low (2 T) field values of the Hall coefficient, respectively. Heavy lines are carrier density changes estimated from the capacitance data using top (n_{c1}) and bottom (n_{c2}) areas. Other lines are guides to the eye.

[16,17]. Thus, charge trapping is a likely scenario for the overestimate of the n_{2d} change from the $C(V_g)$ data, and thus we rely on the Hall data as a direct probe of the free carrier density in the electron gas.

Next, we focus on the change in electron mobility, which is independent of the weak Hall effect nonlinearity. Using the standard Hall mobility formula $\mu_H = (en_{2d}R)^{-1}$ where e is the electronic charge, $\mu_H(V_g)$ was calculated. The μ_H data are shown in Fig. 3, together with $n_{2d}(V_g)$. These results show a clear and consistent reduction of the electron mobility as V_g decreases from 100 to -50 V, at $T = 100$ mK. This change is a factor of 9.3 (8 T Hall coefficient data), with a similar change at $T = 2$ K. Thus, in this system, the change in conductivity is dominated by the mobility change, and not the sheet carrier density, which varies by a factor of only $\sim$1.8 in the same V_g range. At even higher temperature ($T = 20$ K, data not shown), we find the same dominance of the mobility change, emphasizing the robustness of this result.

We have modeled the carrier distribution assuming a triangular well with the $LaAlO_3$ acting as an infinite potential barrier at the origin [18]. We use the band structure assumptions of Ueno *et al.* [6], i.e., that the three doubly degenerated conduction band valleys centered at the Γ point of $SrTiO_3$ show no bandsplitting, and consists of one heavier mass band (effective mass of $m_h^\star = 4.8m_0$, where m_0 is the bare mass) and two lighter bands ($m_l^\star = 1.2m_0$). At $V_g = 0$, we take a self-consistent average electric field as the confining potential. This is nonlinear in the carrier density, as given by $E_{\rm av} = A[\exp(0.5eBn_{2d}\varepsilon_0^{-1}) - 1]$, where ε_0 is the vacuum permittivity, $A = 8.349 \times 10^4$ V/m, and $B = 4.907 \times 10^{-10}$ m/V [17]. Using the 2 K high field value of $n_{2d} = 2.0 \times 10^{13}$ cm^{-2}, we find an effective relative permittivity $\varepsilon_r \sim 1.5 \times 10^4$ and $E_{\rm av} \sim 1.2 \times 10^5$ V/m.

In this approximation, the solutions of the Schrödinger equation are Airy functions of the form $\zeta_i(z) = Ai\{z\alpha - [1.5\pi(i - 0.25)]^{2/3}\}$, where $\alpha = (\hbar^2/2m^\star eE_{\rm av})^{1/3}$, z is the direction normal to the interface, and i is an integer. Electrons are added progressively into the energy bands until the total charge n_{2d} is reached, and the Fermi energy E_F is determined self consistently. The electron distribution can then be calculated using the eigenenergies E_i for $E_i < E_F$, and the corresponding wave functions ζ_i using

$$n_{3d}(z) = \sum_{j=l,h}\left(\frac{g_j m_j^\star}{2\pi\hbar^2}\sum_i (E_F - E_i)|\zeta_i(z)|^2\right) \tag{1}$$

with $g_h = 2$, $g_l = 4$, and $E_i = eE_{\rm av}\alpha^{-1}[1.5\pi(i - 0.25)]^{2/3}$. The result of this calculation gives an electron distribution as shown in the inset of Fig. 4. The peak volume carrier density $n_{3d}^{\rm max} = 1.3 \times 10^{19}$ cm^{-3} is well within the range of densities for which superconductivity in bulk $SrTiO_3$ is found [19].

To give a real space picture of the physics occurring when applying finite V_g, we must consider two effects.

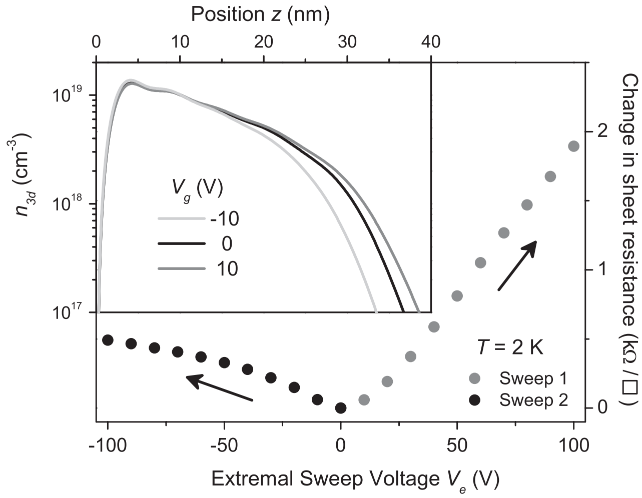

FIG. 4. Sheet resistance at $V_g = 0$ V and $T = 2$ K after applying an extremal voltage V_e. Sweep two was performed after resetting the system at $T = 300$ K. Inset: Electron distribution calculations at three bias voltages.

First, the insulating $SrTiO_3$ substrate acts as simply a capacitor which moves charge to the interface. The electric field $E_{\rm av}$ confining this charge will then change with n_{2d} according to the previous nonlinear equation. However, at the same time, the conduction and valence bands of the bulk $SrTiO_3$ must be connected continuously with those of the metallic gas. Thus, for $V_g < 0$ ($V_g > 0$), an additional compression (expansion) of the electron gas will occur due to band bending, similar to previous discussions in the case of mobility suppression in gated n-AlGaAs-GaAs heterojunctions [20]. Qualitatively, we can illustrate the effect of this bias using the above model in a small voltage range ($\pm$10 V). We add the nonlinear $E_{\rm av}$ and the applied electric field due to V_g to define the new confining potential [18] and recalculate the electron distribution for n_{2d} interpolated at $V_g = \pm 10$ V. These data are also shown in the inset of Fig. 4, and clearly demonstrate the compression (expansion) effect with negative (positive) gate bias.

In this range, V_g is a small perturbation on $E_{\rm av}$. At larger V_g, a fully self-consistent calculation is necessary to incorporate the local nonlinear permittivity $\varepsilon_r(V_g, z)$ [16,17]. Although very computationally demanding, the response of the electron distribution and lattice relaxation effects must also be included [21] in order to achieve a full quantitative understanding of the gating effect. The inclusion of nonlinearities of the permittivity tend to collapse the value ε_r close to the interface, leading to further compression of the gas closer to the $LaAlO_3/SrTiO_3$ interface [22], and may even counterintuitively increase $n_{3d}^{\rm max}$ at large negative biases. As noted above, the superconductivity in our sample shows a much more sensitive response to an applied voltage than the previous study, where T_c could be suppressed to zero only in the regime $V_g < 0$. Also, our maximum in T_c is larger than that of Ref. [2], despite our lower starting value of n_{2d}. This contrast is therefore not due simply to the different sheet carrier densities in the system, but rather it depends on the detailed density distribution $n_{3d}(z)$. This is critical for understanding the superconducting phase diagram and is not universal in the presence of nonlinearities in ε_r.

The decrease of the mobility is thus correlated with the loss of the lower density "tail" region of the $n_{3d}(z)$ distribution, and an increased relative contribution of interface scattering at the $LaAlO_3/SrTiO_3$ interface as the center of mass of the electron gas moves closer to the $LaAlO_3$. Additionally, any decrease in ε_r will enhance the scattering cross section of previously screened ionized impurities, and compound the mobility reduction of the electron gas. This result has important implications when discussing the suppression of the superconducting state since changes in the disorder must be considered in addition to the change in n_{2d}.

In this sample, a relatively weak but clear nonlinearity in the Hall effect measurement was found (Fig. 2). In brief, this Hall effect nonlinearity can be caused by multiple parallel conduction paths with different electron mobilities, or possibly by magnetic contributions. The former cause is more likely in the general case and would naturally arise due to the concomitant distribution of the mobility and electron density throughout the thickness of $SrTiO_3$. The reduction of the Hall effect nonlinearity for larger negative gate voltages is then a natural consequence of the loss of the low carrier density, higher mobility tail of the electron distribution. The increased electric field squeezes the electron distribution further towards the $LaAlO_3/SrTiO_3$ interface, homogenizing the mobility distribution.

Finally, we briefly discuss history effects associated with irreversible changes in the resistance at low temperatures as V_g is swept. These changes can only be removed by warming to room temperature. The main panel Fig. 4 shows how the change in R at ($V_g = 0$) behaves as a function of the previous extremal voltage applied. That is to say, we applied V_g to a maximum positive (or negative) value of V_e, again set $V_g = 0$, and then measured R. First, V_e was ramped from 0 to -100 V in 10 V steps. After this, the sample was warmed to 300 K to reset the system, and cooled again to 2 K, and V_e was then ramped from 0 to $+100$ V.

A clear asymmetry in $R(V_e)$ is found: positive V_e induces a much larger differential increase in R than negative V_e. Such an asymmetry may be understood via the discussion above concerning the distortion of the electron distribution by the gate voltage. Positive V_g, extending the electron distribution deeper into the $SrTiO_3$ substrate, causes electrons to fall into previously unfilled trap states. After the gate voltage is removed, and when the emission rate from the trap states is low, the system does not return to the previous state, but at a higher resistance, as observed. For $V_g < 0$, the electrons are pressed closer to the $LaAlO_3$ layer, but a significant number of new traps are not revealed, consistent with the asymmetry of the resistance change shown in Fig. 4. The increase in resistance for $V_g < 0$ is then assigned to additional charge trapping due to interfacial ferroelectricity [23], the presence of which is suggested by the capacitance data already discussed.

In conclusion, we have studied the EFE at the $LaAlO_3/SrTiO_3$ interface, and have shown that the electron mobility plays a dominant role in controlling the conductivity of this system. These data are consistent with a distortion of the electron wave function towards the interface. Thus, variations in the effective disorder may dominate the modulation of the superconducting transition, which in our case could be suppressed to $T_c = 0$ K using both positive and negative gate voltages. Moreover, we expect that these changes in electron scattering will generally be present when using the EFE to tune any superconductor-insulator transition, evidence for which has been noted elsewhere [12,24].

We thank M. Lippmaa for use of cleanroom facilities and A. M. Goldman for useful discussions. C. B. acknowledges partial funding from the Canon Foundation in Europe, and B. G. K. the National Core Research Center program of Pusan National University [R15-2006-02-01002-0(2008)].

[1] C. H. Ahn *et al.*, Rev. Mod. Phys. **78**, 1185 (2006).
[2] A. D. Caviglia *et al.*, Nature (London) **456**, 624 (2008).
[3] K. A. Parendo *et al.*, Phys. Rev. Lett. **94**, 197004 (2005).
[4] H. Nakamura *et al.*, Appl. Phys. Lett. **89**, 133504 (2006).
[5] S. Thiel *et al.*, Science **313**, 1942 (2006).
[6] K. Ueno *et al.*, Nature Mater. **7**, 855 (2008).
[7] N. Reyren *et al.*, Science **317**, 1196 (2007).
[8] A. Ohtomo and H. Y. Hwang, Nature (London) **427**, 423 (2004).
[9] N. Nakagawa, H. Y. Hwang, and D. A. Muller, Nature Mater. **5**, 204 (2006).
[10] M. Basletic *et al.*, Nature Mater. **7**, 621 (2008).
[11] A. Brinkman *et al.*, Nature Mater. **6**, 493 (2007).
[12] K. A. Parendo *et al.*, Phys. Rev. B **73**, 174527 (2006).
[13] D. Matthey *et al.*, Phys. Rev. Lett. **98**, 057002 (2007).
[14] M. Salluzzo *et al.*, Phys. Rev. Lett. **100**, 056810 (2008).
[15] C. Bell *et al.*, Appl. Phys. Lett. **94**, 222111 (2009).
[16] A. Saifi and L. E. Cross, Phys. Rev. B **2**, 677 (1970).
[17] R. C. Neville, B. Hoeneisen, and C. A. Mead, J. Appl. Phys. **43**, 2124 (1972).
[18] F. Stern, Phys. Rev. B **5**, 4891 (1972).
[19] C. S. Koonce *et al.*, Phys. Rev. **163**, 380 (1967).
[20] K. Hirakawa, H. Sakaki, and J. Yoshino, Phys. Rev. Lett. **54**, 1279 (1985).
[21] D. R. Hamann, D. A. Muller, and H. Y. Hwang, Phys. Rev. B **73**, 195403 (2006).
[22] T. Susaki, N. Nakagawa, and H. Y. Hwang, Phys. Rev. B **75**, 104409 (2007).
[23] R. Zuleeg and H. H. Wieder, Solid State Electron. **9**, 657 (1966).
[24] A. M. Goldman (private communication).